Remote Sensing of Environment 324 (2025) 114747

Contents lists available at ScienceDirect

Remote Sensing of Environment

journal homepage: www.elsevier.com/locate/rse

Rainfall-caused water film on canopy surface biases remotely-sensed vegetation greenness

Si Gao [a], Kai Yan [a,*], Guangjian Yan [a], Miina Rautiainen [b], Yuri Knyazikhin [c], Ranga B. Myneni [c]

[a] State Key Laboratory of Remote Sensing and Digital Earth, Faculty of Geographical Science, Beijing Normal University, Beijing 100875, China
[b] School of Engineering, Aalto University, Espoo 00076, Finland
[c] Department of Earth and Environment, Boston University, Boston, MA 02215, USA.

ARTICLE INFO

Edited by Jing M. Chen

Keywords:
Water film
Precipitation
Vegetation greenness
Vegetation indices (VI)
Data collaboration

ABSTRACT

Remotely-sensed vegetation greenness exhibits obvious differences before and after the short-term heavy rainfall event. This short communication reports that residual water film on the canopy caused by precipitation directly affects the spectral signal of vegetation, which in turn biases observed vegetation greenness. We combined ground measurements, unmanned aerial vehicle (UAV) measurements, three-dimensional radiative transfer model (RTM) simulations, and satellite observations to assess this phenomenon and investigate the impact of water film on vegetation indices (VIs) across different scales and vegetation types. Our findings demonstrate that precipitation exerts a quick and significant influence on the spectral characteristics of canopy components. The presence of water can lead to reflectance attenuation in soil and vegetation components across the entire visible and infrared spectrum, particularly in the near-infrared (NIR) band, with reductions of up to 0.12. The reduction in VI measures after precipitation can be explained by an imbalance in the magnitude of visible and NIR reflectance attenuation caused by the canopy water film. Taking the difference vegetation index (DVI) as an example, the decrease in NIR reflectance is more pronounced than that of red reflectance in the presence of water, resulting in DVI decreasing after a rainfall event. Satellite observations indicated that NDVI and EVI could decrease even exceeding 0.3 in some pixels after short-term rainfall. This work reveals the water film as a possible factor contributing to the bias between true and observed vegetation greenness. The spatial distribution of rainfall seasonality exhibits variation across different regions worldwide, and mitigating the impact of water film on vegetation greenness is essential for enhancing the precision and reliability of global vegetation dynamics monitoring.

1. Introduction

Vegetation plays a crucial role in terrestrial ecosystems, linking the atmosphere, soil, and water, and is extensively studied due to its sensitivity to climate change (Gordon, 2008; Sellers, 1985). Precisely assessing vegetation status and its spatial and temporal dynamics holds significant scientific and practical importance. Remote sensing has emerged as an essential tool for tracking the structural and physiological processes of vegetation due to its ability to take repeatable measurements over large spatial and temporal scales. Identifying the impact of climate change on vegetation growth along with the mechanisms driving it has become a hot issue in global environmental change research. Satellite data reveals that since the 1980s, global vegetation has increased, with 52 % to 59 % of areas showing longer growing season length and higher leaf area index (LAI) (Piao et al., 2020). In 2023, 63 % of global vegetation continued this greening trend, according to the latest records of normalized difference vegetation index (NDVI) (Li et al., 2024). Scholars have gradually reached a consensus on the phenomenon of "global greening" under climate change and human activities (Atkinson et al., 2011; Chen et al., 2019a; Forzieri et al., 2020; Ukkola et al., 2021; Zhu et al., 2022).

Despite extensive research on vegetation and climate change, uncertainty persists in accurately representing vegetation greenness, dynamics, and their underlying drivers. Greenness is commonly characterized using vegetation indices (VIs), the most popular remotely-sensed indicators derived from mathematical operations on spectral reflectance (Huete, 2014). Ideally, A reliable "greenness proxy" for VI should be a composite measure of vegetation leaf abundance,

* Corresponding author.
E-mail address: kaiyan@bnu.edu.cn (K. Yan).

https://doi.org/10.1016/j.rse.2025.114747
Received 22 August 2024; Received in revised form 14 March 2025; Accepted 4 April 2025

biochemical traits and pigment, independent of non-vegetative factors. However, satellite-measured spectral reflectance is determined by various factors like component optical properties, canopy structures, sun-sensor geometries, and atmospheric conditions, leading to biases between VI-informed greenness and true greenness (Gao et al., 2024; Samanta et al., 2012; Zeng et al., 2023). A large number of studies showed that aerosols (Christensen et al., 2017; Xiao et al., 2003; Zhang et al., 2023) and sun-sensor geometries (Maeda and Galvão, 2015; Norris and Walker, 2020) affect satellite-observed vegetation greenness. Furthermore, even surface reflectance cannot fully eliminate interference from non-vegetative factors. Dust accumulation on leaf surfaces has received some attention in small-scale vegetation studies in mining and urban areas (Kończak et al., 2021; Ma et al., 2023), as it can distort vegetation spectra instantly, and influence photosynthetic efficiency and growth over time.

By contrast, rainfall has a greater impact on greenness measurement because the spatial and temporal patterns of rainfall intensity and frequency vary widely from local to global scales. Most studies have focused on the long-term effects of rainfall on vegetation greenness, and little attention has been paid to short-term changes in spectra and greenness caused by rainfall trapped in vegetation pixels, which motivated our study. Fig. 1 presents a schematic illustration of our hypothesis. Initially, clear sky condition allows successful satellite observation. In the second stage, rainfall can be intercepted by the canopy, evaporated, infiltrated into the soil, or run off along the slope when rainfall intensity exceeds the infiltration rate. In the third stage, a clear sky returns, permitting satellite observation, but a water film remains on the vegetation pixel. Without considering physical canopy damage from prolonged extreme rainfall or resulting pigment changes, the disparity in clear-sky greenness observations between post-precipitation (Stage 3) and pre-precipitation (Stage 1) can be attributed to the presence of a residual canopy water film. The water film on leaves, branches, trunks, and soil alters component spectra and VI values, inevitably introducing uncertainties in greenness detection that are difficult to quantify and cannot be mitigated through conventional methods such as atmospheric corrections. Notably, canopy interception accounts for approximately 30 % of total precipitation, with forests alone contributing 11–48 % of rainfall redistribution due to high evapotranspiration rates (Ferreira Rodrigues et al., 2021; Murakami, 2021). However, even though researchers have a vague awareness of the fact that water affects observation signals, the impact of water film on observed greenness has not been fully appreciated.

Combining the previous hypothesis with rainfall characteristics, we can deduce that water film, as an unavoidable environmental factor, has systematic and random influences on vegetation greenness assessment. Systematic impacts are primarily manifested through seasonal precipitation regimes, as exemplified by the cyclical alternation of wet and dry seasons in tropical rainforests, which may induce systematic seasonal biases in observed greenness. Random effects stem from the spatio-temporal variability of rainfall events (intensity, duration, and distribution patterns), generating non-stationary noise through post-precipitation moisture residues in remote sensing signals. These unpredictable residuals may instantly alter leaf optical properties, thereby disrupting vegetation physiology assessments, especially for short-term processes like diurnal fluctuation in photosynthesis and respiration. In summary, rainfall events would introduce both systematic and random biases to remote sensing observations, potentially leading to erroneous interpretations of seasonal vegetation dynamics while introducing complexities into vegetation modeling processes. Furthermore, global warming has intensified the hydrological cycle, leading to changes in rainfall patterns with more frequent extreme rainfall events (Ham et al., 2023), thus placing greater demands on accurate estimates of greenness and highlighting the need to elucidate the mechanistic process by which water influences the signals of remotely sensed observations.

This short communication reveals that the water film is a possible factor contributing to the bias between true greenness and observed greenness. We combined ground-observed spectra, three-dimensional (3D) radiative transfer (RT) model simulations, unmanned aerial vehicle (UAV), and satellite observations to compare the greenness with/without water film disturbance across different scales and types of vegetation. The primary purpose of this research is to bring the issue of rainfall-caused water film bias remotely-sensed greenness to the attention of ecological researchers.

2. Data and methods

2.1. Rationale for water affecting vegetation greenness

The surface reflectance of remotely-sensed observations depends on the spectral characteristics of the components within the pixel. The spectral reflectance curve of vegetation exhibits a pronounced absorption feature in the red band and a strong reflection feature in the near-infrared (NIR) band, resulting in a significant difference between the two bands. The soil reflectance is relatively flat and consistent across the

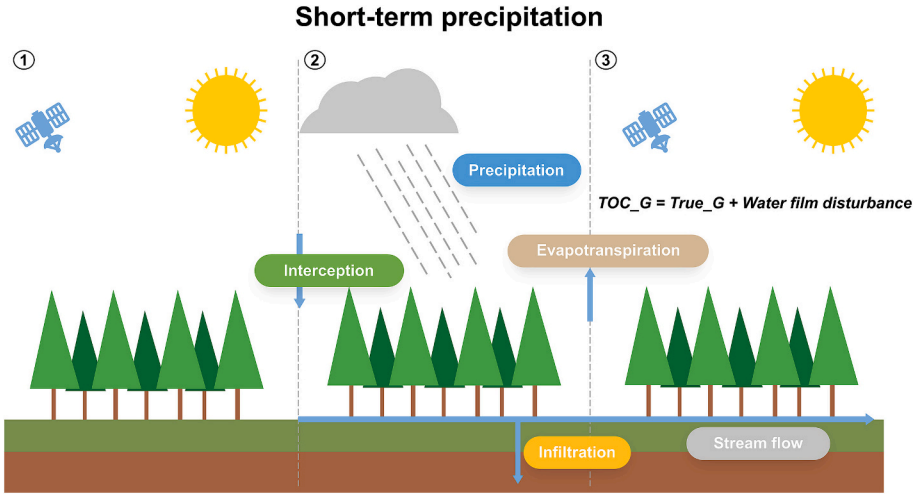

Fig. 1. Schematic of how short-term rainfall affects the signals observed by satellites. TOC_G represents the greenness at the top of the canopy, i.e., observed greenness. True_G indicates the true greenness. Water film disturbance refers to the effect of residual rainfall (e.g., water film on the leaves, branches, and soil) on the observed greenness under the clear sky after the rainfall event. This process overlooks the physical damage to the canopy structure caused by rainfall due to the brief time interval.

visible (VIS) and NIR spectra. Water absorbs strongly in all bands, with the most significant reflection occurring in the blue band (Fig. 2(a)). When a rainfall event occurs, following the fundamental principle that the component spectra comprise the canopy spectrum, we hypothesize that the canopy reflectance with a water film exhibits a gradual decrease across the full VIS-NIR spectrum, particularly in the NIR band. Accordingly, the difference between NIR and red band reflectance will decrease, and the reflection-absorption angle will increase. Moreover, in theory, difference vegetation index (DVI) (Roujean and Breon, 1995), simple ratio (SR) (Jordan, 1969), and normalized difference vegetation index (NDVI) (Rouse et al., 1974) would also decrease, as indicated by the formula (Fig. 2(b)).

2.2. Experiments using ground measurements, RT simulations, UAV measurements, and satellite observations

This study employed ground measurements, 3D RT simulations, UAV, and satellite observations to verify the hypothesis that residual water films from rainfall affect observed greenness. First, ground-based measurements were conducted on a fine scale (component, crown, canopy) to assess the impact of water on the spectral characteristics of vegetation in the absence of significant external disturbances. Second, based on the measured spectra, wet and dry Aspen monocultures with varying LAIs were simulated using the large-scale remote sensing data and image simulation framework (LESS) model (Qi et al., 2019, 2022, 2023) to explore the effect of water films on greenness at different vegetation densities. The UAV measurements and satellite experiments aimed to confirm the effect of short-term precipitation on remotely-sensed greenness (i.e., VI values) at a regional level. The combination of ground measurement, UAV measurement, 3D RT simulations, and satellite observations is expected to verify our hypotheses from leaf scale to crown, canopy, and regional scale. The specific details are described as follows.

2.2.1. Ground measurements

Ground measurements took place from June 11–13, 2023, at Huailai remote sensing experimental station in Hebei Province, China (40.349°N, 115.788°E). We conducted a control experiment with two scenarios: one with untreated, dry conditions and another where the canopy surface was sprayed with tap water to simulate post-precipitation, keeping the leaves and soil moist. Hyperspectral reflectance measurements of peach, pine, corn, and grass canopies, with and without water film disturbance, were collected at nadir from an approximate height of 1 m above the canopies using a hand-held ASD

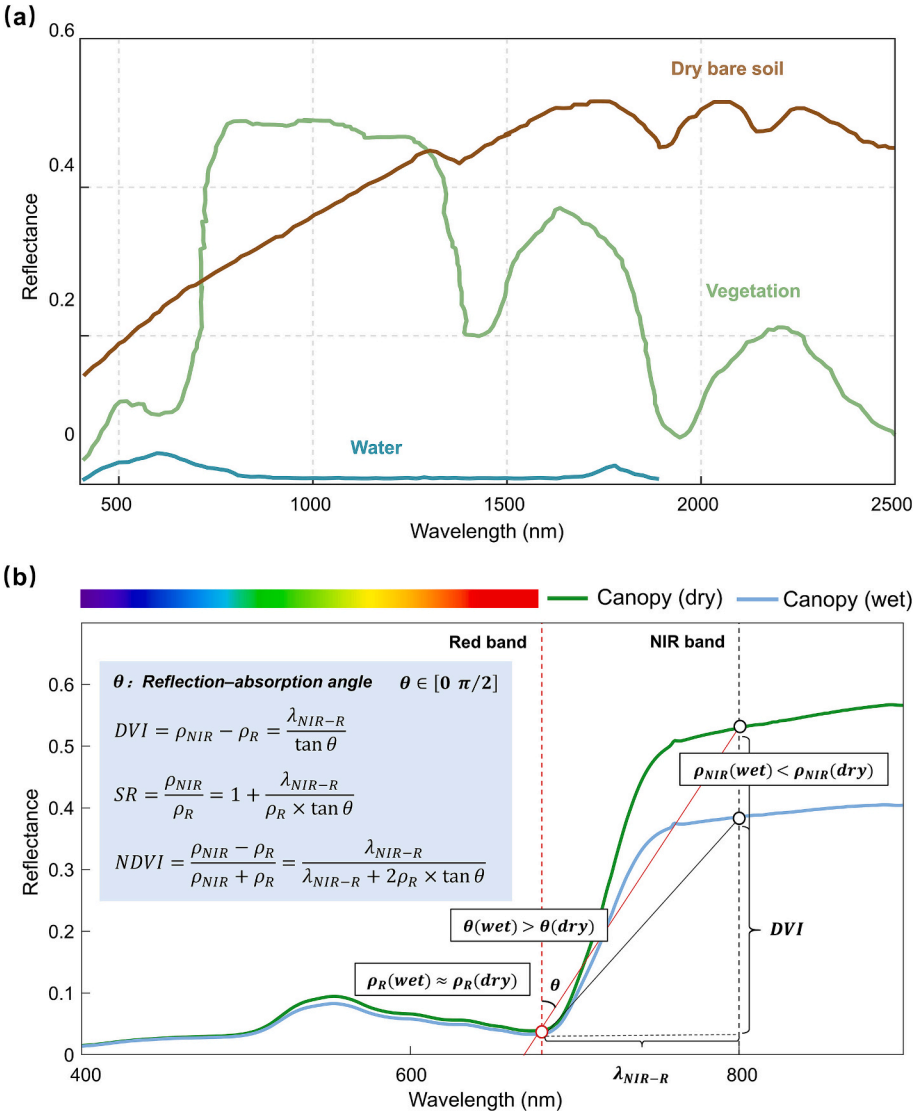

Fig. 2. Principle of how water affects observed greenness. (a) Typical spectral reflectance of water, vegetation, and soil components (Chiu, 2005). (b) Canopy reflectance and the theoretical derivation of vegetation indices with and without the water film disturbance.

FieldSpec 3 spectroradiometer (Analytical Spectral Devices, Boulder, CO, USA). Subsequently, we collected Aspen leaf samples and measured their spectra, both with and without water film, using a leaf clip with an internal halogen light source attached to a plant probe. We also collected dry and wet soil samples below the location of the Aspen samples and measured their corresponding spectra with a soil probe (Fig. 3(a)). On the day of sampling and measurements, the weather was mostly sunny with occasional cloud cover, no rain, and 32–48 % humidity. All spectral measurements were taken in triplicate with similar results.

Additionally, on November 3, 2024, we conducted an indoor experiment with a miniature *Pachira aquatica* landscape to simulate five rainfall levels: dry (0 mm), small (10 mm), moderate (25 mm), large (50 mm), and extreme large rainfall (200 mm). We used an ASD FieldSpec 4 spectroradiometer to measure the leaf and soil spectra, observing the impact of varying rainfall levels on these components.

2.2.2. LESS model simulations

To investigate the effect of water on vegetation at different densities, we employed the LESS model (Qi et al., 2019, 2022) to construct Aspen monocultures with varying LAIs ranging from 0 to 7 with increments of 0.25. Bidirectional reflectance factors (BRFs) for pre/post-precipitation scenarios were simulated based on the measured component spectra of dry and wet Aspen leaves and soil, utilizing a leaf clip attachment and soil probe (Fig. 3(b)). To create realistic forests, the individual tree model (OBJ format file) of Aspen was generated using OnyxTREE software (https://www.onyxtree.com/). The simulated scenes measured 30 m by 30 m, with Aspen trees uniformly distributed. The solar azimuth angle (SAA), view azimuth angle (VAA), and view zenith angle (VZA) were all set to 0°, while the solar zenith angle (SZA) was set to 30°. All simulations were conducted at 2 nm intervals across the 400–1000 nm range. We combined the spectral response functions (SRFs) of the Sentinel-2 Multispectral Instrument (MSI) sensor with the simulated continuous spectrum to calculate broadband reflectance.

2.2.3. UAV imagery acquisition

The rainfall record at Hailai Station indicated that the short-term rainfall event began at 20:20 on July 24, 2024, and ended at 9:00 on July 25, accumulating 35 mm. UAV hyperspectral images before and after rainfall were captured using an X20P-IR hyperspectral imager (Cubert GmbH, Ulm, Baden-Württemberg, Germany) mounted on the DJI M300RTK UAV platform (SZ DJI Technology Co., Shenzhen, China) (Fig. 3(c)). The device captures hyperspectral images across over 160 spectral channels, covering the 350–1000 nm range at high speed. Its high-performance sensor minimizes noise, and the dual GigE camera interface supports a frame rate of up to 5 Hz (1886*1886 pixels/frame). The pre-precipitation image was captured at 10:15 on July 24, 2024, with SZA/SAA of 54.7°/115.6°, respectively. The post-precipitation image was taken at 13:14 on July 25, 2024, with SZA/SAA of 65.7°/215.4°. The UAV flew at an altitude of 100 m, with a heading overlap of 80 % and a side overlap of 70 %.

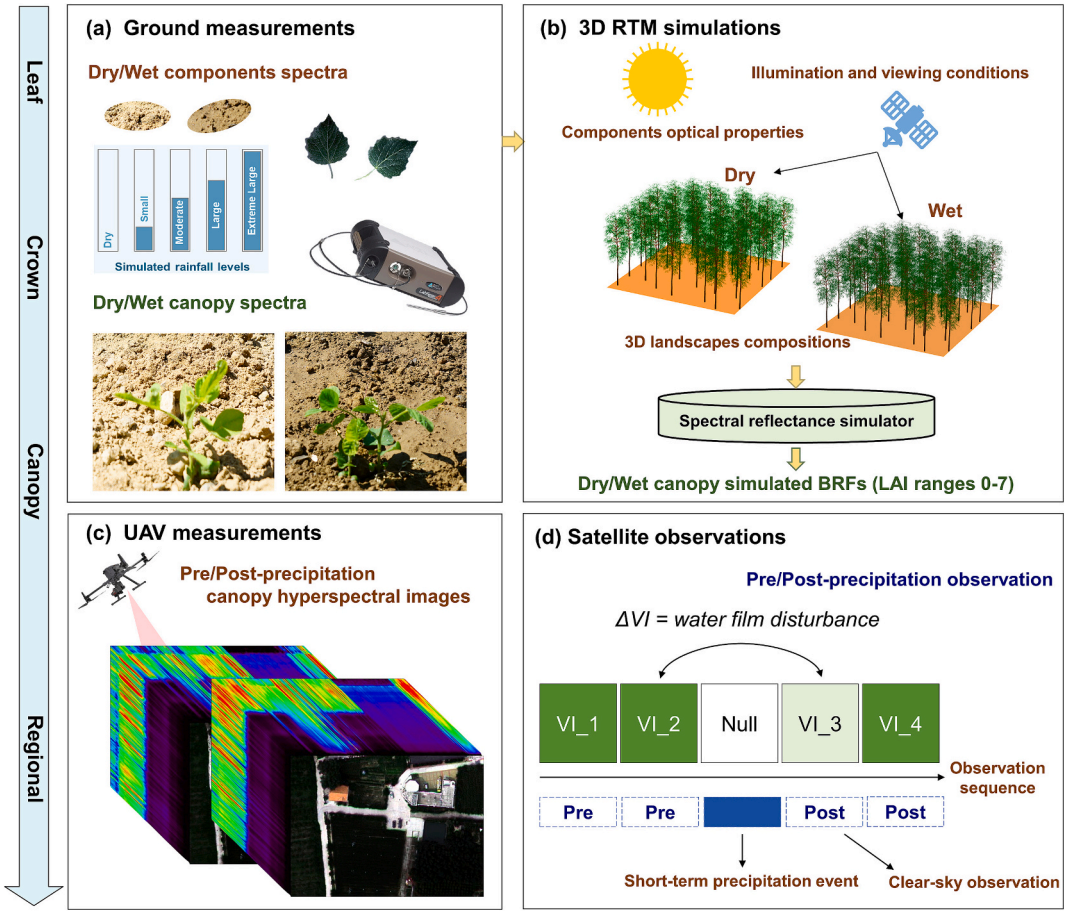

Fig. 3. Flowchart of adopted research methodology. (a) Ground-based measurements involved using an ASD spectrometer to capture outdoor low-canopy, soil, and leaf spectra in dry and wet conditions, as well as indoor soil and leaf spectra under simulated rainfall. (b) A 3D RT model simulates wet and dry Aspen monocultures with varying LAIs using outdoor measurements of Aspen leaf and soil spectra. (c) UAV hyperspectral measurements were taken at Huailai on July 24, 2024, before and after a short-term precipitation event. (d) Satellite data were analyzed for comparisons before and after the rain and for time-series mutation tests. VI_n denotes the vegetation index for a specific day.

2.2.4. Satellite observations

The satellite images of NDVI and enhanced vegetation index (EVI) (Huete, 1997) were generated using reflectance datasets MOD09GA (https://lpdaac.usgs.gov/products/ mod09gav061/) from the moderate-resolution imaging spectroradiometer (MODIS) for the period spanning June 1, 2020, to July 31, 2020. Two sets of VI images, one with water film disturbance and the other without, were captured within a 8-day time window to ensure consistent true greenness (Fig. 3(d)). We randomly selected five global plots representing different vegetation ecosystems — forests, savannas, grasslands, croplands, and shrublands. These plots, located between −27.29° and 41.96°N latitude and 84.61° and 121.67°E longitude, span temperate, tropical, and subtropical climates with diverse precipitation patterns. This selection ensures spatial representativeness and global reliability of the results. To evaluate the impact of rainfall on vegetation greenness over time, we performed a time-series mutation analysis on the June 2020 VIs time series and the cumulative rainfall data from the preceding day at a randomly selected point within the Australian shrublands.

Land cover data were sourced from the MODIS MCD12Q1 product (Sulla-Menashe and Friedl, 2022), which provides an annual land cover classification map with a spatial resolution of 500 m. Daily rainfall data were derived from the ECMWF ERA5 datasets (https://www.ecmwf.int/en/forecasts/dataset/ecmwf-reanalysis-v5), which provide aggregated precipitation values for each day. To enhance data credibility, several quality control procedures were applied to detect and discard poor-quality data. Land cover maps were used to restrict the study area to vegetation pixels only. The quality assurance (QA) band identified and removed poor-quality observations, such as clouds, cloud shadows, and adjacent masks of clouds and snow. Additionally, we considered only pixels acquired at VZAs below 40°.

3. Results

3.1. Ground-measured results

Ground-based measurements of canopy spectra show that for all vegetation types, the spectral characteristics of the canopy change with and without water film (Fig. 4). In the VIS-NIR spectral region, the wavelengths exhibiting the most pronounced variations in reflectance between dry and wet conditions are all located in the NIR bands (996 nm for peach, 893 nm for pine, 947 nm for corn, and 999 nm for grass), with corresponding differences of 0.13, 0.06, 0.06, and 0.18, respectively. In the VIS domain, the largest difference in canopy reflectance between dry and wet conditions was only 0.02 (peach, 549 nm).

The comparison of spectral reflectance of leaf and soil components across various rainfall classes reveals that the spectral reflectance of these components significantly decreased across all bands following rainfall, with spectral differences tending to saturate as rainfall increased (Fig. 5). The extreme difference (maximum reflectance – minimum reflectance) for leaves across different rainfall levels was highest in the NIR band, approximately 0.12, and lower in the visible and short-wave infrared (SWIR) bands, all below 0.08. For soil, the extreme difference in the NIR band was also about 0.12, with even greater differences in the SWIR band, reaching up to 0.25. The spectral reflectance of both leaves and soil approached saturation as rainfall levels increased, with leaves reaching saturation more rapidly than soil. This difference in saturation behavior can be attributed to the contrasting water-holding capacities of leaves and soil. Leaves, with their relatively limited surface area and internal structure, reach their maximum water retention capacity more quickly than soil, which, depending on its texture and composition (e.g., clay content, organic matter), can absorb and retain a significantly larger volume of water before reaching saturation.

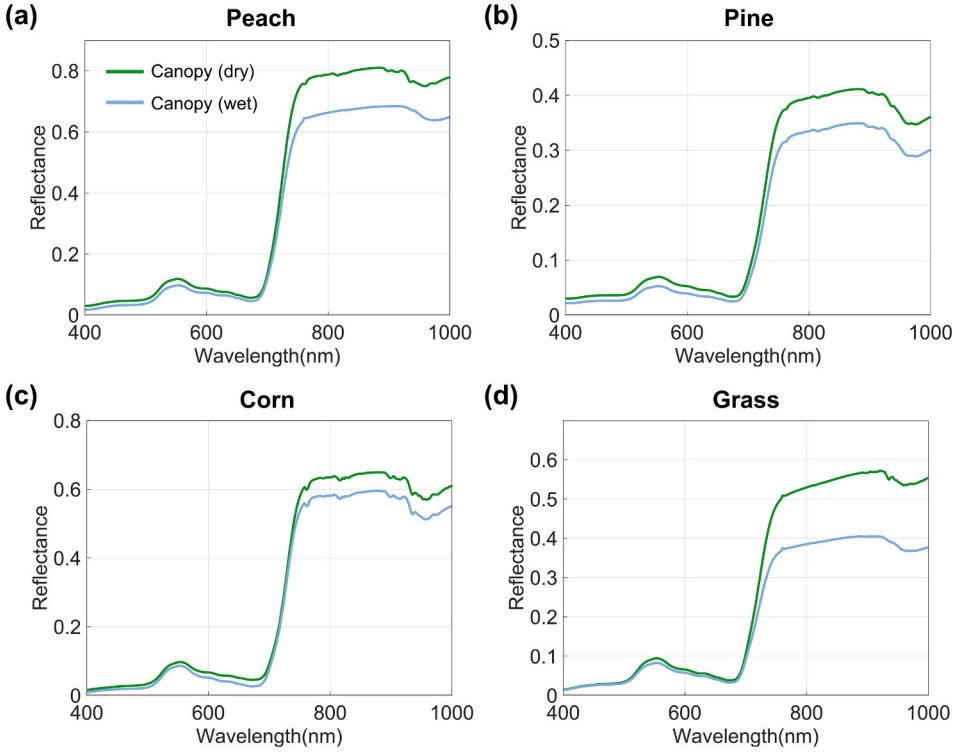

Fig. 4. Canopy spectral reflectance with and without water film disturbance, as measured on the ground using a hand-held ASD FieldSpec 3 Hi-Res portable object spectroradiometer.

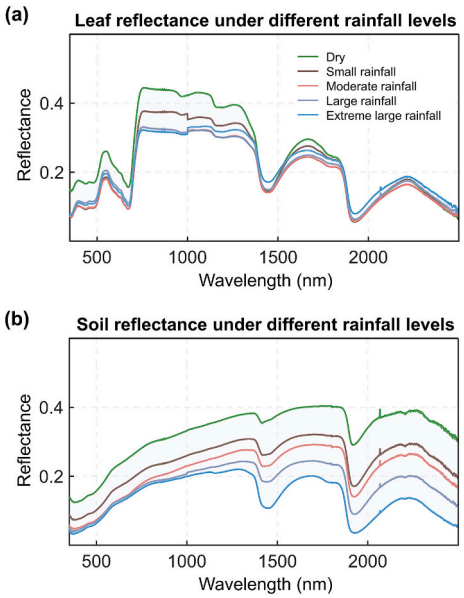

Fig. 5. Components spectral reflectance under different rainfall levels, measured indoors using a leaf clip and soil probe with an ASD FieldSpec spectrometer.

3.2. Simulated results

Fig. 6 displays the component spectra, simulated canopy BRFs, and Sentinel-2 MSI reflectance for Aspen monocultures across various LAI scenarios, comparing dry and wet conditions. Wet leaf/soil reflectance was significantly lower than dry conditions across all bands, with the most pronounced reduction in the NIR band. Under the same LAI conditions, the BRFs of dry Aspen consistently exceed those of wet Aspen. The differences between wet and dry conditions were particularly pronounced in the NIR, Red-edge 2, and Red-edge 3 bands. Paired reflectance points (dry vs. wet canopy) across bands consistently plot below the 1:1 line; with increasing LAI, reflectance approaches saturation, and the disparity between wet and dry conditions diminishes. This phenomenon is likely due to the dominant influence of soil water on canopy characteristics in sparse canopies, while leaf surface water plays a more critical role in dense canopies.

3.3. UAV results

The UAV hyperspectral imaging results reveal a marked decrease in spectral reflectance for both Aspen and Corn plots after rainfall, particularly in the NIR band (Fig. 7). Reflectance at 678, 478, and 802 nm, as shown in the paired density scatter plots comparing pre- and post-rainfall conditions, typically falls below the 1:1 line. Rainfall offsets the NIR reflectance change by about 0.1, underscoring its substantial influence on vegetation's spectral properties.

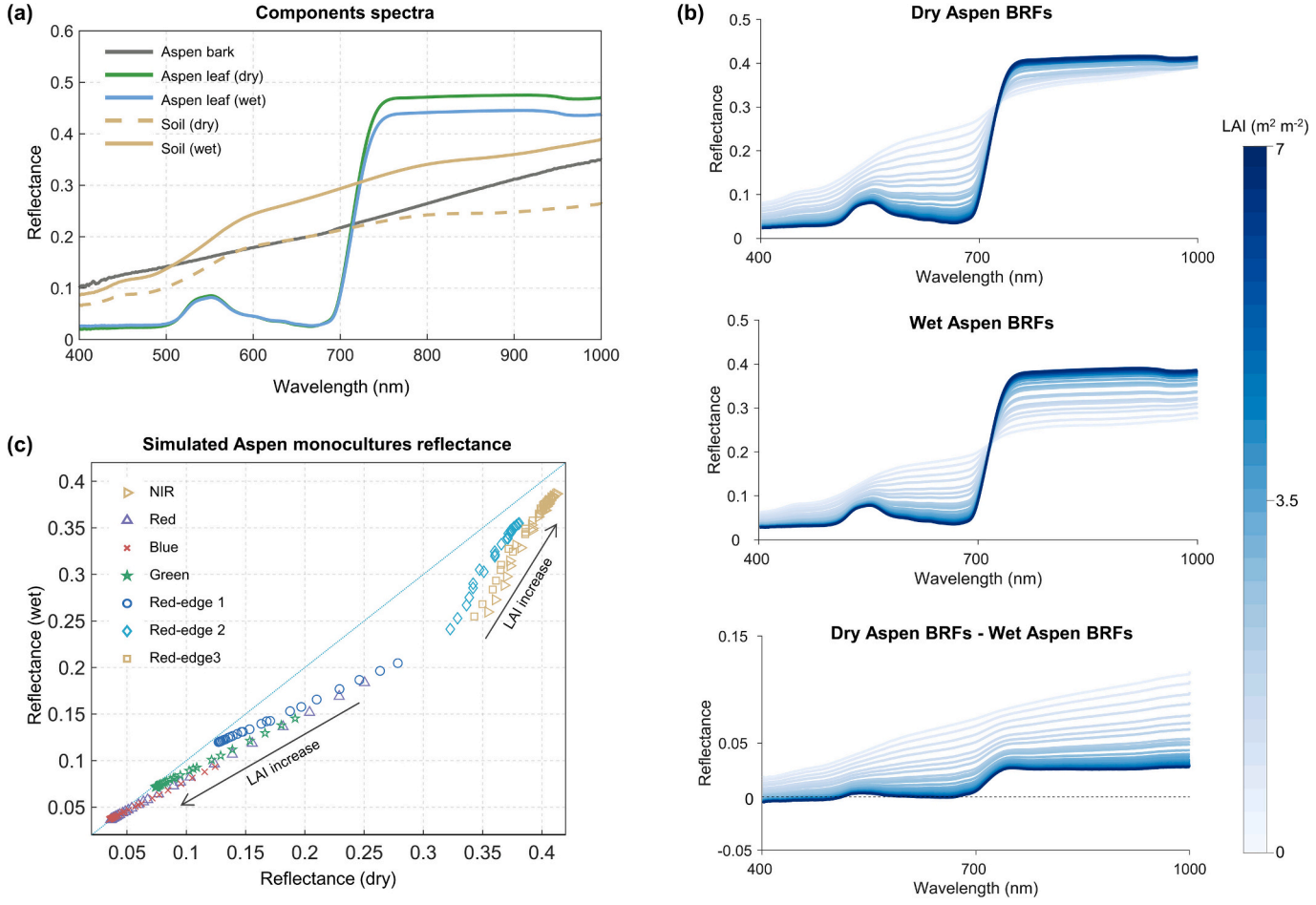

Fig. 6. Input data for the LESS model and simulation results include: (a) the optical properties of leaf, bark, and soil components of an Aspen stand, measured on the ground; (b) canopy spectral reflectance of Aspen monocultures under dry and wet conditions, simulated using the LESS model; (c) simulated Sentinel-2 MSI reflectance for both wet and dry Aspen scenes.

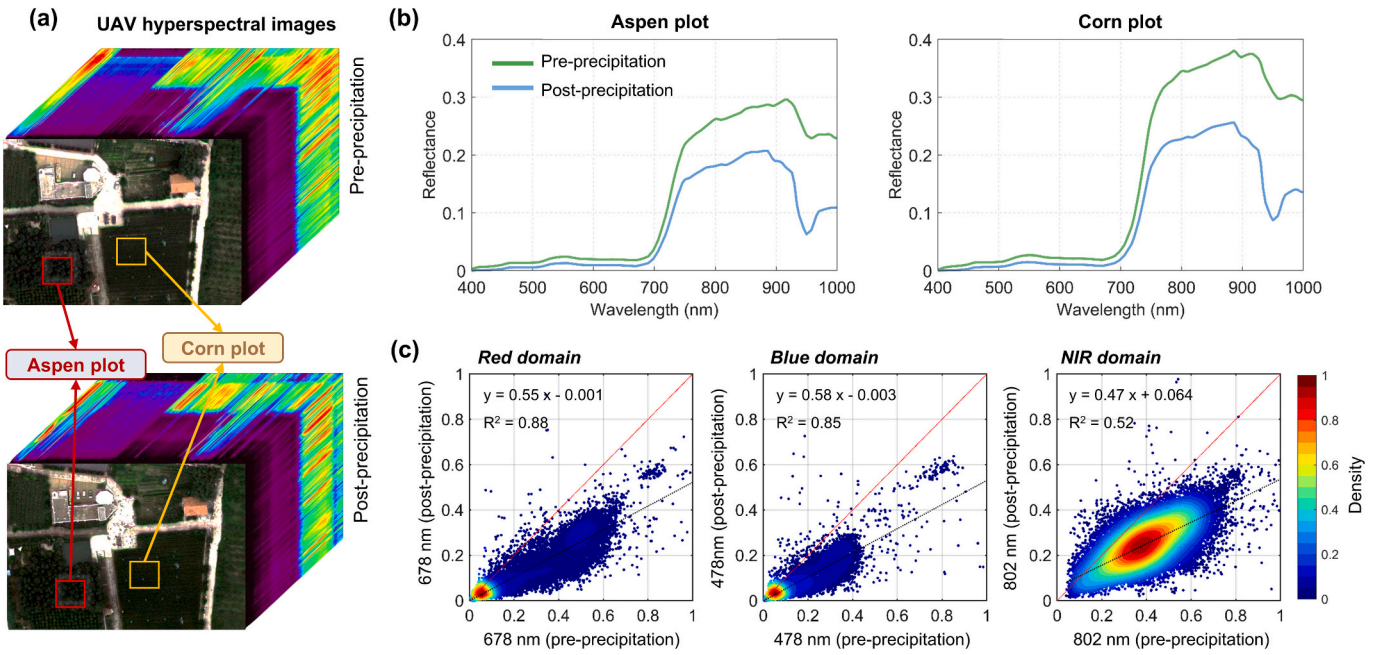

Fig. 7. UAV-based observations: (a) hyperspectral images captured by UAV before and after rainfall; (b) spectral reflectance of Aspen and Corn plots pre- and post-rainfall; (c) scatter density plots comparing spectral reflectance at 678, 478, and 802 nm pre- and post-precipitation.

3.4. Satellite observed results

By comparing the VIs images affected and not affected by short-term heavy rainfall, it can be observed that for all vegetation types, the VIs values show a significant decrease post-precipitation, with NDVI being more affected (Fig. 8). The reduction of EVI and NDVI by short-term heavy rainfall can even exceed 0.3 in some pixels. In addition, we found that rainfall also affects the spatial heterogeneity of the canopy greenness and that different VIs affect it to different extents. Fig. 9 shows that the precipitation events occurring on June 11, 12, and 18

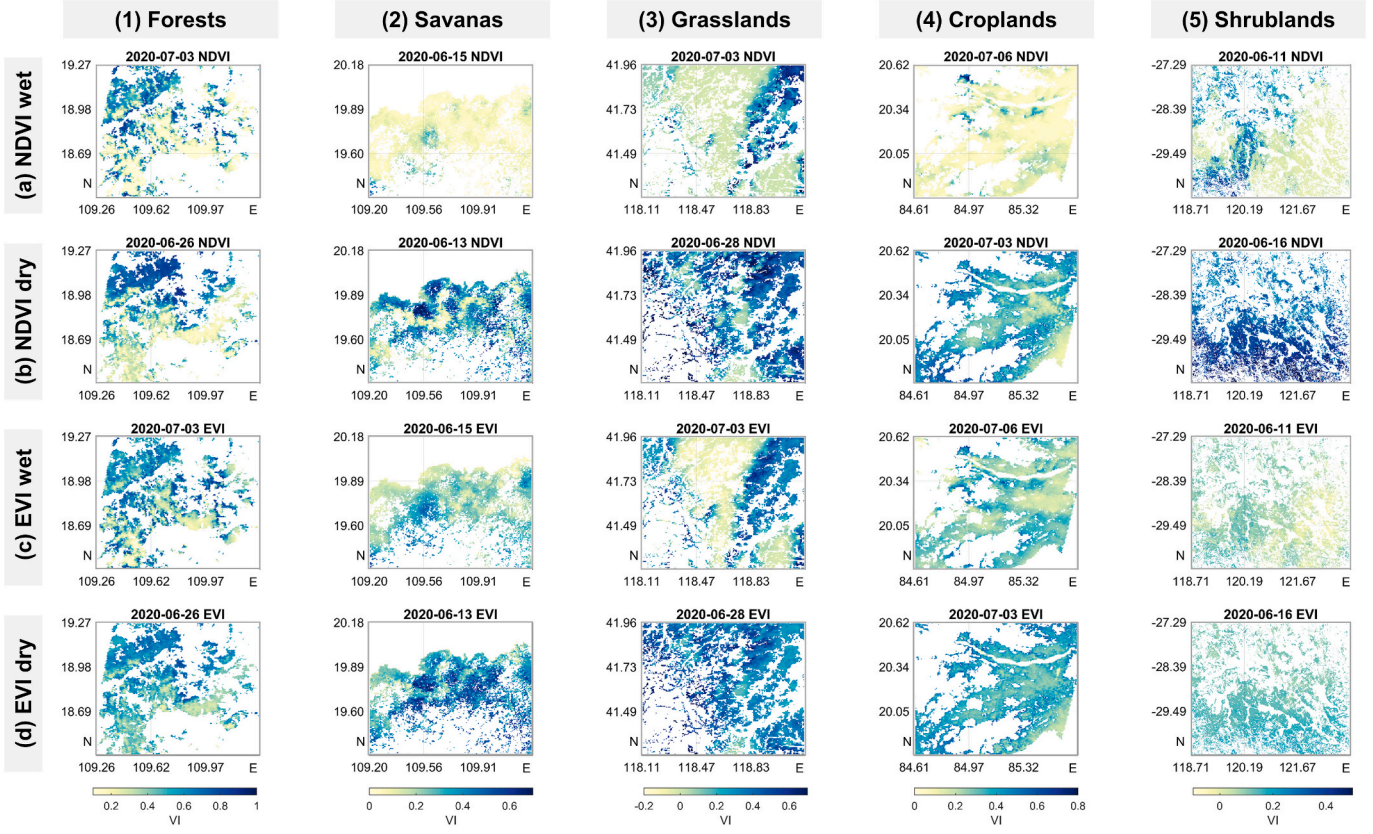

Fig. 8. Comparison of MODIS NDVI and EVI images for various vegetation type plots, with (wet) and without (dry) short-term heavy rainfall impact. The cumulative rainfall amount during this event was 45, 48, 66, 27, and 20 mm for forests, savannas, grasslands, croplands, and shrublands, respectively.

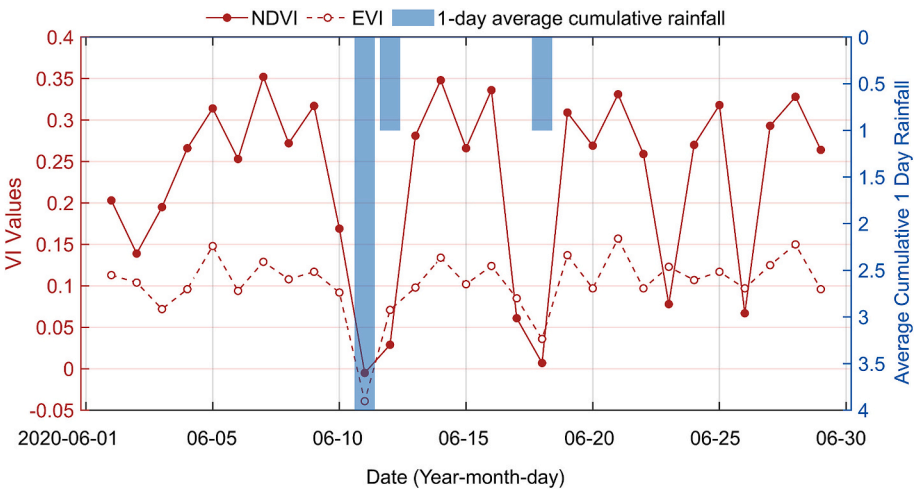

Fig. 9. Comparison of the time series of NDVI and EVI for one point in the shrub sample plot in June 2020 with the time series of cumulative rainfall during the previous day.

substantially contributed to the underestimation of NDVI and EVI, with similar levels of underestimation (NDVI decreasing by about 0.3 and EVI by about 0.15) on each day. This indicates that even non-intense precipitation can notably decrease the greenness of low canopy like shrublands.

4. Discussion

This study combined ground, UAV, 3D RT simulation, and satellite data to assess the effects of water films on observed signals of vegetation across scales. Ground-based measurements revealed spectral changes in leaf/soil components and low canopies, while UAV and satellite data provided landscape-level insights. Although the general trends observed across these scales were consistent (i.e., decreased spectral reflectance and VI values after rainfall), the magnitude of these changes varied. For instance, the maximum reduction in NIR reflectance observed at the leaf level was more pronounced than the changes observed in the UAV observation, which may be attributed to several factors, including differences in rainfall amount, observational conditions and sensor, scale effect, and mixed-pixel problem.

While water film as an unavoidable environmental factor, exerting both systematic and random effects on vegetation greenness, is easy to understand, current ecological research often ignores this bias, potentially leading to erroneous conclusions or misinterpretations. Only strikingly fewer studies pointed out in the discussion that the presence of a water film on leaf surfaces may decrease greenness estimates because water reflects strongly in red (blue) relative to NIR (Samanta et al., 2012). Our findings reveal that the presence of a water film can lead to a significant 0.3 decrease in NDVI (a regional average decrease of over 25 %), which is considerably more pronounced than the approximately 5 % NDVI reduction caused by drought (Chen et al., 2019b). However, in vegetation greenness trend analyses, VIs fluctuations are typically attributed to vegetation physiography or atmospheric artifacts, neglecting the influence of water storage at the canopy-soil interface.

Rainfall-induced water films introduce systematic and random biases into various aspects of vegetation monitoring. First, rainfall phenology may affect the observed greenness phenology. For example, tropical regions are generally divided into wet and dry seasons. During the wet season, the contribution of rainfall signals is greater, which may lead to an underestimation of the observed greenness, which in turn misinterpret the greenness difference between the dry and wet seasons. Secondly, rainfall phenology varies considerably in different regions, resulting in spatial differences in greenness observation conditions, which may amplify the spatial heterogeneity of greenness monitoring. Furthermore, variations in the attributes of rainfall events, such as rainfall depth, duration, and inter-event intervals, significantly influence the degree of water impact on vegetation greenness, especially on a diurnal cycle. Climate change is projected to increase precipitation variability globally (Feldman et al., 2024a, 2024b; Konapala et al., 2020). Regions with distinct wet and dry seasons are expected to experience amplified fluctuations between precipitation and evapotranspiration, while areas with consistent rainfall throughout the year may face intensified wet seasons. This increased variability will exacerbate the interference of water films on VIs, highlighting the necessity of quantifying, modeling, and ultimately mitigating this phenomenon.

While the present study has elucidated the impact of water film on canopy reflectance and VIs from a mechanistic standpoint and verified this hypothesis through ground measurements, RTM simulations, UAV, and satellite observations, there are limitations in both the theoretical derivation and the validation processes. In the theoretical analysis, we used the position of the narrow band instead of the wide band when setting the reflection-absorption angle, concluding that DVI, NDVI, and SR that incorporated both VIS-NIR bands would decrease due to water effects. However, the bandwidth and mathematical form could substantially affect VI values and patterns (Gao et al., 2023; Liang et al., 2020). Ground-based measurements can be optimally integrated with data obtained from UAVs to provide a broader perspective. As for satellite observations, unlike ground measurements and simulations that can control variables effectively, it is difficult to completely remove atmospheric effects even with strict quality control (Christensen et al., 2017). Therefore, it is difficult to interpret whether the greenness bias observed by satellites is the effect of canopy water film or water vapor, aerosol, and thin clouds. Additionally, our assumptions do not consider alterations in the actual greenness of the surface attributable to precipitation events; e.g., substantial rainfall may disrupt the canopy structure, and vegetation regulates internal physiological systems and pigment content instantly in response to a short-term precipitation event. In the future, a larger sample of UAV data, geostationary satellite data and RT modeling with the raindrop introduction would be helpful in better quantifying the short-term effects of rainfall on vegetation greenness.

The challenge for our study is to quantify the effect of rainfall-induced water film on greenness. The interception process of canopy and litter trapped in the underlying surface consists of three phases: the dampening phase, the steady saturation phase, and the post-rainfall drainage phase, and their durations vary considerably (Li et al., 2016). Furthermore, the interception was in turn controlled by three sets of variables: (1) rainfall characteristics, such as rainfall intensity and total

precipitation; (2) canopy structural characteristics, such as leaf area and leaf morphology; (3) meteorological parameters, such as wind speed, relative humidity (Gerrits and Savenije, 2011). These circumstances make interpreting the water film effect based on satellite observations practically impossible. Using imagery data from multiple sunny days can mitigate the impact of water films on remote sensing signals, but this strategy becomes unavailable when studying ecological phenomena at small spatial and temporal scales. There is an urgent need to develop new VI that are insensitive to water films yet capable of reflecting vegetation greenness. Combining a vegetation RT model coupled with water droplets with a watershed hydrological process simulation model may be a feasible solution.

5. Conclusions

This short communication uncovered the phenomenon that rainfall-caused water film on the canopy surface biases remotely-sensed vegetation greenness. By integrating ground-based spectral measurements, three-dimensional (3D) radiative transfer (RT) simulations, unmanned aerial vehicle (UAV) measurements, and satellite observations, we have demonstrated that residual water significantly influences the canopy spectral characteristics and, consequently, the derived vegetation indices (VIs). The findings indicate that the decrease in post-precipitation VIs is primarily attributed to the differential attenuation of visible and near-infrared reflectance by the remaining water film on vegetation organs and soil. Our study also underscores the importance of considering the spatial and temporal variability of rainfall in assessing vegetation greenness. In future research, we would continue to quantify the water film effect on canopy greenness to enhance the precision and reliability of global vegetation dynamics monitoring.

CRediT authorship contribution statement

Si Gao: Writing – original draft, Visualization, Software, Methodology, Conceptualization. **Kai Yan:** Writing – review & editing, Project administration, Methodology, Funding acquisition. **Guangjian Yan:** Methodology, Funding acquisition, Formal analysis. **Miina Rautiainen:** Writing – review & editing, Supervision, Resources. **Yuri Knyazikhin:** Writing – review & editing, Supervision, Resources. **Ranga B. Myneni:** Writing – review & editing, Supervision, Resources.

Declaration of competing interest

The authors declare that they have no known competing financial interests or personal relationships that could have appeared to influence the work reported in this paper.

Acknowledgments

This work was supported by the National Natural Science Foundation of China (Grant No. 42271356). We are grateful to Anzhou Technology Co. Ltd. (Beijing, China) for UAV operational support. We also appreciate the editor and anonymous reviewers' constructive comments and suggestions, which helped improve the entire work and manuscript.

Data availability

Data will be made available on request.

References

Atkinson, P.M., Dash, J., Jeganathan, C., 2011. Amazon vegetation greenness as measured by satellite sensors over the last decade. Geophys. Res. Lett. 38. https://doi.org/10.1029/2011GL049118.

Chen, C., Park, T., Wang, X., Piao, S., Xu, B., Chaturvedi, R.K., Fuchs, R., Brovkin, V., Ciais, P., Fensholt, R., Tømmervik, H., Bala, G., Zhu, Z., Nemani, R.R., Myneni, R.B., 2019a. China and India lead in greening of the world through land-use management. Nat. Sustain. 2, 122–129. https://doi.org/10.1038/s41893-019-0220-7.

Chen, X., Mo, X., Zhang, Y., Sun, Z., Liu, Y., Hu, S., Liu, S., 2019b. Drought detection and assessment with solar-induced chlorophyll fluorescence in summer maize growth period over North China plain. Ecol. Indic. 104, 347–356. https://doi.org/10.1016/j.ecolind.2019.05.017.

Chiu, W.-Y., 2005. Wetland Mapping through Semivariogram Guided Fuzzy Segmentation of Multispectral Satellite Imagery. University of Calgary, Department of Geomatics Engineering.

Christensen, M.W., Neubauer, D., Poulsen, C.A., Thomas, G.E., McGarragh, G.R., Povey, A.C., Proud, S.R., Grainger, R.G., 2017. Unveiling aerosol–cloud interactions – part 1: cloud contamination in satellite products enhances the aerosol indirect forcing estimate. Atmos. Chem. Phys. 17, 13151–13164. https://doi.org/10.5194/acp-17-13151-2017.

Feldman, A.F., Feng, X., Felton, A.J., Konings, A.G., Knapp, A.K., Biederman, J.A., Poulter, B., 2024a. Plant responses to changing rainfall frequency and intensity. Nat. Rev. Earth Environ. https://doi.org/10.1038/s43017-024-00534-0.

Feldman, A.F., Konings, A.G., Gentine, P., Cattry, M., Wang, L., Smith, W.K., Biederman, J.A., Chatterjee, A., Joiner, J., Poulter, B., 2024b. Large global-scale vegetation sensitivity to daily rainfall variability. Nature 636, 380–384. https://doi.org/10.1038/s41586-024-08232-z.

Ferreira Rodrigues, A., Rogério de Mello, C., Nehren, U., de Coimbra, Pedro, Ribeiro, J., Alves Mantovani, V., Marcio de Mello, J., 2021. Modeling canopy interception under drought conditions: the relevance of evaporation and extra sources of energy. J. Environ. Manag. 292, 112710. https://doi.org/10.1016/j.jenvman.2021.112710.

Forzieri, G., Miralles, D.G., Ciais, P., Alkama, R., Ryu, Y., Duveiller, G., Zhang, K., Robertson, E., Kautz, M., Martens, B., Jiang, C., Arneth, A., Georgievski, G., Li, W., Ceccherini, G., Anthoni, P., Lawrence, P., Wiltshire, A., Pongratz, J., Piao, S., Sitch, S., Goll, D.S., Arora, V.K., Lienert, S., Lombardozzi, D., Kato, E., Nabel, J.E.M. S., Tian, H., Friedlingstein, P., Cescatti, A., 2020. Increased control of vegetation on global terrestrial energy fluxes. Nat. Clim. Chang. 10, 356–362. https://doi.org/10.1038/s41558-020-0717-0.

Gao, Si, Zhong, R., Yan, K., Ma, X., Chen, X., Pu, J., Gao, Sicong, Qi, J., Yin, G., Myneni, R.B., 2023. Evaluating the saturation effect of vegetation indices in forests using 3D radiative transfer simulations and satellite observations. Remote Sens. Environ. 295, 113665. https://doi.org/10.1016/j.rse.2023.113665.

Gao, S., Yan, K., Liu, J., Pu, J., Zou, D., Qi, J., Mu, X., Yan, G., 2024. Assessment of remote-sensed vegetation indices for estimating forest chlorophyll concentration. Ecol. Indic. 162, 112001. https://doi.org/10.1016/j.ecolind.2024.112001.

Gerrits, A.M.J., Savenije, H.H.G., 2011. Forest floor interception. In: Forest Hydrology and Biogeochemistry: Synthesis of Past Research and Future Directions. Springer, pp. 445–454.

Gordon, B.B., 2008. Forests and climate change: forcings, feedbacks, and the climate benefits of forests. Science 320, 1444.

Ham, Y.G., Kim, J.H., Min, S.K., Kim, D., Li, T., Timmermann, A., Stuecker, M.F., 2023. Anthropogenic fingerprints in daily precipitation revealed by deep learning. Nature 622, 301–307. https://doi.org/10.1038/s41586-023-06474-x.

Huete, A., 1997. A comparison of vegetation indices over a global set of TM images for EOS-MODIS. Remote Sens. Environ. 59, 440–451. https://doi.org/10.1016/S0034-4257(96)00112-5.

Huete, A., 2014. Vegetation indices. In: Encyclopedia of Earth Sciences Series, pp. 883–886. https://doi.org/10.1007/978-0-387-36699-9_187.

Jordan, C.F., 1969. Derivation of leaf-area index from quality of light on the forest floor. Ecology 50, 663–666. https://doi.org/10.2307/1936256.

Konapala, G., Mishra, A.K., Wada, Y., Mann, M.E., 2020. Climate change will affect global water availability through compounding changes in seasonal precipitation and evaporation. Nat. Commun. 11. https://doi.org/10.1038/s41467-020-16757-w.

Kończak, B., Cempa, M., Pierzchała, Ł., Deska, M., 2021. Assessment of the ability of roadside vegetation to remove particulate matter from the urban air. Environ. Pollut. 268, 115465. https://doi.org/10.1016/j.envpol.2020.115465.

Li, X., Xiao, Q., Niu, J., Dymond, S., van Doorn, N.S., Yu, X., Xie, B., Lv, X., Zhang, K., Li, J., 2016. Process-based rainfall interception by small trees in northern China: the effect of rainfall traits and crown structure characteristics. Agric. For. Meteorol. 218–219, 65–73. https://doi.org/10.1016/j.agrformet.2015.11.017.

Li, X., Wang, K., Huntingford, C., Zhu, Z., Peñuelas, J., Myneni, R.B., Piao, S., 2024. Vegetation greenness in 2023. Nat. Rev. Earth Environ. 5, 241–243. https://doi.org/10.1038/s43017-024-00543-z.

Liang, L., Huang, T., Di, L., Geng, D., Yan, J., Wang, S., Wang, L., Li, L., Chen, B., Kang, J., 2020. Influence of different bandwidths on LAI estimation using vegetation indices. IEEE J. Sel. Top. Appl. Earth Obs. Remote Sens. 13, 1494–1502. https://doi.org/10.1109/JSTARS.2020.2984608.

Ma, B., Yang, X., Che, D., Shu, Y., Liu, Q., Su, M., 2023. Spectral simulation and error analysis of dusty leaves by fusing the Hapke two-layer medium model and the linear spectral mixing model. Remote Sens. 15, 1220. https://doi.org/10.3390/rs15051220.

Maeda, E.E., Galvão, L.S., 2015. Sun-sensor geometry effects on vegetation index anomalies in the Amazon rainforest. GIsci. Remote Sens. 52, 332–343. https://doi.org/10.1080/15481603.2015.1038428.

Murakami, S., 2021. Water and energy balance of canopy interception as evidence of splash droplet evaporation hypothesis. Hydrol. Sci. J. 66, 1248–1264. https://doi.org/10.1080/02626667.2021.1924378.

Norris, J.R., Walker, J.J., 2020. Solar and sensor geometry, not vegetation response, drive satellite NDVI phenology in widespread ecosystems of the western United States. Remote Sens. Environ. 249, 112013. https://doi.org/10.1016/j.rse.2020.112013.

Piao, S., Wang, X., Park, T., Chen, C., Lian, X., He, Y., Bjerke, J.W., Chen, A., Ciais, P., Tømmervik, H., Nemani, R.R., Myneni, R.B., 2020. Characteristics, drivers and feedbacks of global greening. Nat. Rev. Earth Environ. https://doi.org/10.1038/s43017-019-0001-x.

Qi, J., Xie, D., Yin, T., Yan, G., Gastellu-Etchegorry, J.P., Li, L., Zhang, W., Mu, X., Norford, L.K., 2019. LESS: LargE-scale remote sensing data and image simulation framework over heterogeneous 3D scenes. Remote Sens. Environ. 221, 695–706. https://doi.org/10.1016/j.rse.2018.11.036.

Qi, J., Xie, D., Jiang, J., Huang, H., 2022. 3D radiative transfer modeling of structurally complex forest canopies through a lightweight boundary-based description of leaf clusters. Remote Sens. Environ. 283, 113301. https://doi.org/10.1016/j.rse.2022.113301.

Qi, J., Jiang, J., Zhou, K., Xie, D., Huang, H., 2023. Fast and accurate simulation of canopy reflectance under wavelength-dependent optical properties using a semi-empirical 3D radiative transfer model. J. Remote Sens. 3 (17). https://doi.org/10.34133/remotesensing.0017.

Roujean, J.-L., Breon, F.-M., 1995. Estimating PAR absorbed by vegetation from bidirectional reflectance measurements. Remote Sens. Environ. 51, 375–384. https://doi.org/10.1016/0034-4257(94)00114-3.

Rouse, J.W., Haas, R.H., Schell, J.A., Deering, D.W., 1974. Monitoring Vegetation Systems in the Great Plains with Erts.

Samanta, A., Knyazikhin, Y., Xu, L., Dickinson, R.E., Fu, R., Costa, M.H., Saatchi, S.S., Nemani, R.R., Myneni, R.B., 2012. Seasonal changes in leaf area of Amazon forests from leaf flushing and abscission. J. Geophys. Res. Biogeosci. 117, 1–13. https://doi.org/10.1029/2011JG001818.

Sellers, P.J., 1985. Canopy reflectance, photosynthesis and transpiration. Int. J. Remote Sens. 6, 1335–1372.

Sulla-Menashe, D., Friedl, M.A., 2022. MODIS Collection 6.1 (C61) Land Cover Type Product User Guide 1 https://doi.org/https://lpdaac.usgs.gov/products/mcd12q1v061/.

Ukkola, A.M., De Kauwe, M.G., Roderick, M.L., Burrell, A., Lehmann, P., Pitman, A.J., 2021. Annual precipitation explains variability in dryland vegetation greenness globally but not locally. Glob. Chang. Biol. 27, 4367–4380. https://doi.org/10.1111/gcb.15729.

Xiao, X., Braswell, B., Zhang, Q., Boles, S., Frolking, S., Moore, B., 2003. Sensitivity of vegetation indices to atmospheric aerosols: continental-scale observations in northern Asia. Remote Sens. Environ. 84, 385–392. https://doi.org/10.1016/S0034-4257(02)00129-3.

Zeng, Y., Hao, D., Park, T., Zhu, P., Huete, A., Myneni, R., Knyazikhin, Y., Qi, J., Nemani, R.R., Li, F., Huang, J., Gao, Y., Li, B., Ji, F., Köhler, P., Frankenberg, C., Berry, J.A., Chen, M., 2023. Structural complexity biases vegetation greenness measures. Nat. Ecol. Evol. 7, 1790–1798. https://doi.org/10.1038/s41559-023-02187-6.

Zhang, Z., Xiong, J., Fan, M., Tao, M., Wang, Q., Bai, Y., 2023. Satellite-observed vegetation responses to aerosols variability. Agric. For. Meteorol. 329, 109278. https://doi.org/10.1016/j.agrformet.2022.109278.

Zhu, P., Burney, J., Chang, J., Jin, Z., Mueller, N.D., Xin, Q., Xu, J., Yu, L., Makowski, D., Ciais, P., 2022. Warming reduces global agricultural production by decreasing cropping frequency and yields. Nat. Clim. Chang. 12, 1016–1023. https://doi.org/10.1038/s41558-022-01492-5.